[1.] Corina Daniela CUNȚAN, [2.]Gabriel Nicolae POPA, [3.]Corina Maria DINIŞ, [4.] Angela IAGĂR

ANALYSIS OF LC SHUNT FILTERS USED FOR SINGLE–PHASE WELDING MACHINE

[1–4.]Politehnica University of Timisoara, Faculty of Engineering Hunedoara, Hunedoara, ROMANIA

Abstract: Harmonics is the most important dynamic component of power quality, which affects the operation of electrical equipment and, at the same time, reduces the power factor. Harmonic sources in power systems are generally associated with nonlinear loads. To analyze the operation of passive filters (LC shunt filter, parallel capacitive filter), five groups of experiments were performed. A non–linear single–phase consumer consisting of a XENTA 90 type manual welding machine was chosen, relevant for both industry and the domestic sector. For the studied consumer, the improvement of the current waveform depends on the values of L, C, the possibility of improving the power factor, which is particularly important for increasing the efficiency of passive filters. Through the appropriate choice of LC shunt filter, a decrease in the deformation regime is obtained, and by increasing the power factor, a decrease in the electricity losses from the electrical networks is obtained.
Keywords: LC shunt filter, welding machine, power factor, harmonics, THD

1. INTRODUCTION

Energy consumption and power quality, which are employed in power engineering, are closely related in both industrial and nonindustrial applications. The power factor and the total harmonic distortion are two crucial power quality indicies that are correlated with the effectiveness of electrical energy for both electrical suppliers and consumers[1–3].

Because of their low initial cost and efficiency, power passive filters (PPFs), which consist of a set of tuned LC filters and/or low–pass filters, are commonly employed to suppress harmonics and improve power factor.[4–11] However, PPFs have the following disadvantages: the source impedance and operating in the transitory regime have a considerable impact on filter quality. Parallel resonance between the source and the PPFs causes the harmonic current to increase at a given frequency on the source side [12,13].

Power quality indices deviate from compatibility standards, resulting in a number of severe implications for producers, system operators, and energy customers. Poor electrical quality is associated with decreased productivity, equipment breakdowns, significant financial losses, and a shorter lifespan for electrical system components and end–use devices, among other things. Electromagnetic disturbances that occur during the operation of energy systems affect almost all the features of the voltage and current waves: frequency, shape, amplitude, and symmetry (in the case of three–phase systems) [14,15].

Harmonics are the most significant and dynamic component of electromagnetic disturbances. Harmonic sources in power systems are typically linked to nonlinear and switched loads (e.g., rectifier, inverter, voltage controller, frequency converter, welding, AC or DC motor drive, switching power supply, fluorescent and LED lamps, static VAR compensators, etc.). In recent years, the power network has been exposed to various harmonic sources, which have direct effects on the sustainability of electrical equipment, such as electric automobiles, wind and solar power stations with distribution systems, direct current conversion and transmission of high voltages, etc. [2]

2. INVERTER TYPE WELDING DEVICES

Block diagram of an inverter power supply

Fig. 1 shows the block diagram of a power source with an inverter, analyzed with its functional blocks.

ISSN 1584 – 2665 (printed version); ISSN 2601 – 2332 (online); ISSN-L 1584 – 2665

The primary rectifier is an uncontrolled single–phase or three–phase bridge type rectifier, depending on the installed power and the output current range of the power source. The mains circuit of the rectifier has varistors connected for protection against accidental overvoltages coming from the mains. In more modern versions of inverter power sources, the input rectifier is equipped with an active filter for improving the power factor (PFC – Power Factor Corrector) [16].

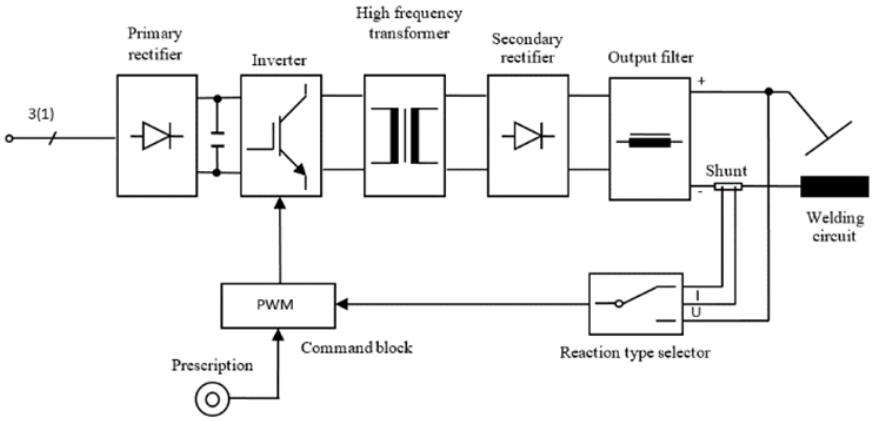

Figure 1. Inverter rectifier welding power source.

Intermediate DC filter is capacitive type and has the role of reducing the rectified voltage ripple that is applied to the inverter. The capacitor is electrolytic type with appropriate nominal voltage and low dielectric losses. For the initial charging of the capacitor at connection, as a rule, an additional circuit with resistors is provided, which is later short–circuited by a contact of an auxiliary relay [16].

The primary inverter block constitutes the primary switching block (high–frequency electronic switching), being implemented with different types of power semiconductor devices, in various topological configurations (forward, half–bridge, bridge). Depending on the type of power semiconductor devices, the circuit topology, as well as the specific output power control requirements, the control of the inverter block is performed through various pulse width modulation strategies (PWM – Pulse Width Modulation).

The high–frequency adaptation transformer is the magnetic component with the role of coupling the circuits (welding with the mains), respectively of power transfer, ensuring both the adaptation of the voltages and the electrical safety of the operator. The construction of the transformer, dictated by considerations of minimizing power losses and dispersion inductance, is made of ferrite cores of different shapes, respectively of windings of stranded wire or copper foil type, in order to reduce additional losses due to eddy currents [16].

The high–frequency secondary rectifier has the role of rectifying the high–frequency alternating voltage in order to feed the direct current welding arc. It is made with ultra–fast rectifier diodes, in different configurations (with median point or single–phase bridge).

The output filter is inductive type and has the role of reducing the variations of the continuous welding current, respectively of ensuring a quick response. Due to the high working frequency, the inductance value is low (μH), the inductance of the connecting conductors related to the welding circuit, also, contributes to smoothing the current.

Analysis of an inverter power source

Fig.2 shows a forward switching converter, implemented with two power transistors, Q1, Q2, with the demagnetization of the core of the transformer T obtained by the half–bridge structure made with diodes D1, D2. The transistors are controlled simultaneously by the control circuit (driver). The voltage on a transistor is half of the value corresponding to the forward topology with a single transistor, namely it is equal to U_d. The maximum filling factor is D_{max}= 0.5. The regulation of the output power is carried out by the PWM regulator, at a constant switching frequency, by changing the filling factor, respectively the conduction time of the transistors [16].

ISSN 1584 – 2665 (printed version); ISSN 2601 – 2332 (online); ISSN-L 1584 – 2665

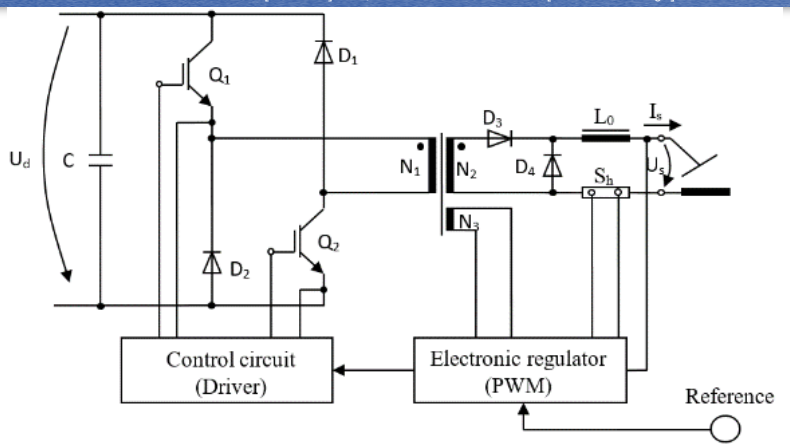

Figure 2. Two–transistor forward structure power supply.

For the physical analysis and experiments, it is chose the XENTA 90 inverter from the ISKRA company, with the following technical data: supply voltage 230 V, maximum power 2.1 kVA, fuse 10 A, power factor cosφ=0.82, output DC, regulated current 5÷ 90 A, maximum electrode 2.5 mm, size 28x15x26 (cm), weight 3.2 kg (Fig.3).

Figure 3. The welding machine XENTA 90.

3. EXPERIMENTAL RESULTS OBTAINED USING THE CA8334B POWER QUALITY ANALYZER

The circuit in Fig. 4.a was made for the purpose of performing experimental measurements (Fig.4.b) to determine the influence of the welding machine on the power supply network.

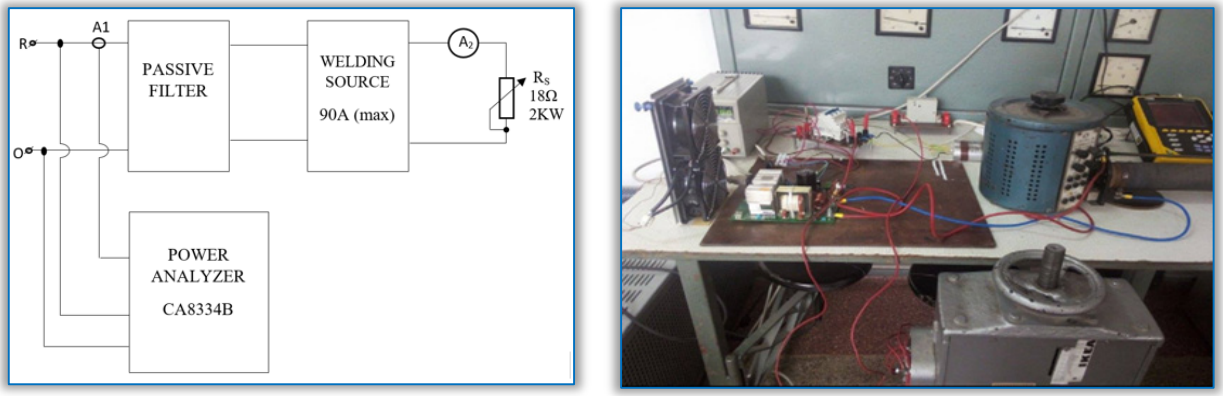

Figure 4. a) Block diagram of the studied circuit; b) Experimental circuit.

- **Results of measurements made when the welding machine (having resistive load) without a passive filter**

Measurements made with the power quality analyzer CA8334B on a welding machine with a load of 18 Ω/2 KW resistor, as can be seen in Table 1, a harmonic distortion factor THD of very high values, which tend to decrease once with the increase of the welding current (I is input AC current; I_s is output DC current) and, implicitly, the current absorbed from the network (Fig.5.a). A relatively low value for the power factor PF is found, slightly above 0.66 and which remains approximately constant with the significant variation of the welding current (Fig.5.d).

ISSN 1584 – 2665 (printed version); ISSN 2601 – 2332 (online); ISSN-L 1584 – 2665

At the same time, the displacement power factor DPF has a small variation when the welding current changes, an inverse variation compared to the power factor PF with the increase of the output current. A higher value for reactive power than active power can be observed for all determined values.

Table 1 – Experimental measurements made with the resistive load welding device: $R_L = 1.5\ \Omega$, without passive filter

I(A)	THD(%)	P(W)	Q(VAR)	S(VA)	PF(–)	DPF(–)	I_s(A)
2.4	105.2	364	410.5	550.3	0.662	0.988	9
3.8	104.5	573.2	655.4	872.4	0.659	0.98	16
5.6	103	827	940	1249	0.66	0.972	23
7.1	98.9	1056	1174	1578	0.67	0.965	30
8.7	95.2	1297	1413	1920	0.676	0.959	37
9.3	93.2	1403	1501	2056	0.683	0.957	42

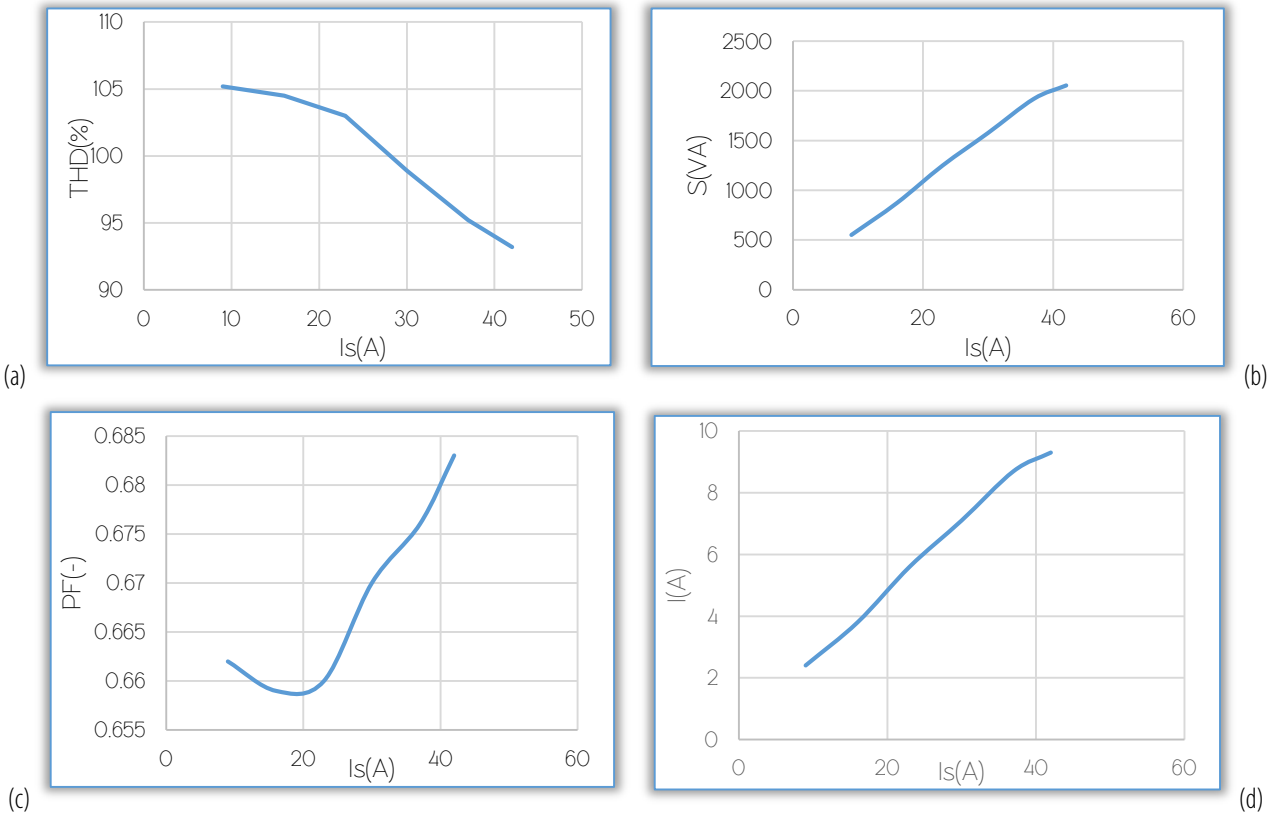

(a) (b) (c) (d)

Figure 5. Graphic representations: a) THD=f(I_s); b) S=f(I_s); c) PF=f(I_s); d) I=f(I_s)

The waveforms for voltage and for current on a period show a shape close to sinusoidal, for voltage with an RMS value of 225 V and a much deformed shape for current with RMS value of 2.4 A (Fig.6.a). This can, also, be seen from the representation of the current harmonics which have the most important values for the lower order ones, and the total harmonic distortion factor THD has a value of over 100%. Fig.6.c shows a relatively reduced phase shift of 9 degrees between voltage and current.

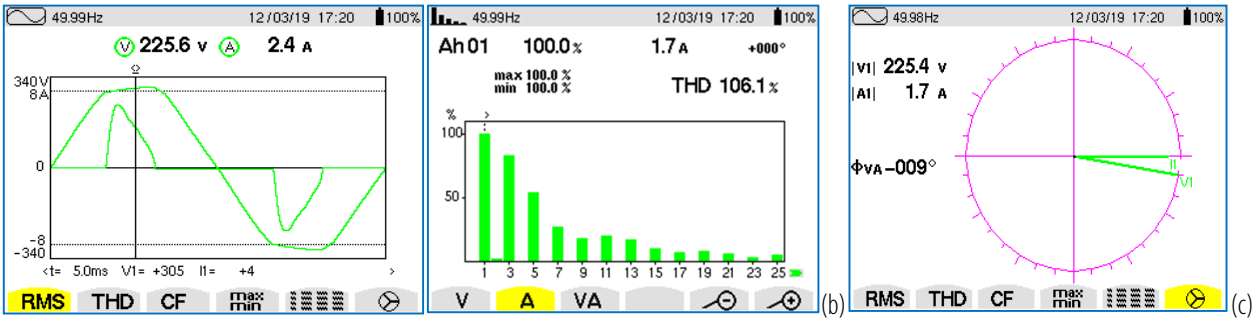

(a) (b) (c)

Figure 6. Measurements with CA 8334B: a) Voltage and current over a period;
b) The harmonic spectrum of the current and the total harmonic distortion factor (THD); c) Fresnel diagram for the fundamental at I_s= 9 A

ISSN 1584 – 2665 (printed version); ISSN 2601 – 2332 (online); ISSN-L 1584 – 2665

The results obtained at a current of 30 A (Fig.7) highlight the same behavior of the welding machine as in the case of a current of 9 A, with the observation of an increase in the phase shift at 15 degrees.

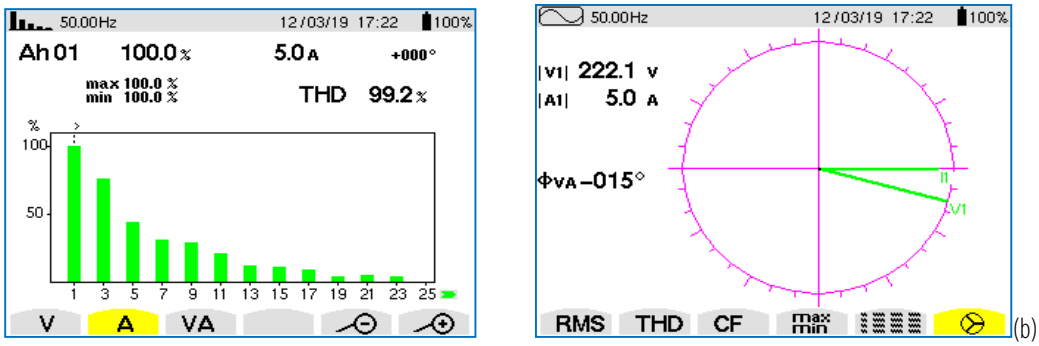

(a) (b)

Figure 7. Measurements with CA 8334B: a) The harmonic spectrum of the current and the total harmonic distortion factor (THD); b) Fresnel diagram for the fundamental at I_s= 30 A

- Results of measurements made when the welding machine (having resistive load) was connected with LC shunt filter (Fig.8)

A variable inductance coil was used: L = 9.1 ÷ 296 mH (with resistance coil R_L). Measurements were made for two values of the LC shunt filter used.

Figure 8. LC shunt filter connected in circuit

- Connecting a LC shunt filter having the characteristics: R_L = 1.5 Ω, L = 271 mH, C = 5 μF and the resonance frequency

From the values listed in Table 2, it can be observed that at the same load current values, the input current changed slightly and the harmonic distortion factor THD decreased by approximately 10 percent. The other presented values did not change significantly, with the active power remaining lower than the reactive power.

$$f = \frac{1}{2\pi\sqrt{LC}} = \frac{1}{2\pi\sqrt{271\cdot10^{-3}\cdot5\cdot10^{-6}}} = \frac{1}{2\pi\sqrt{271\cdot5\cdot10^{-9}}} = 136.72\text{Hz} \quad (1)$$

The displacement factor DPF has an inverse variation compared to the previous situation, meaning its value increases with the increase in output current. The representations of the waveforms for voltage and current in Fig. 9 and 10 do not show significant changes compared to the situation without a filter at the input. The total harmonic distortion (THD) factor, the waveforms, and the phase shift are similar to those in the previously presented situation (Fig. 9).

Table 2–Experimental measurements made with the resistive load connected to welding machine, with LC shunt filter: R_L = 1.5 Ω, L = 271 mH, C = 5 μF

I(A)	THD(%)	P(W)	Q(VAR)	S(VA)	PF(–)	DPF(–)	I_S(A)
2.5	93.8	351	402.8	536	0.654	0.919	9
4.1	96.7	598.5	685	907.5	0.659	0.937	16
5.7	96.2	829	938	1253	0.662	0.942	23
7.5	93.9	1092	1211	1632	0.670	0.939	30
8.7	91	1256	1375	1854	0.676	0.938	37
9.6	88.3	1424	1524	2086	0.683	0.936	42

ISSN 1584 – 2665 (printed version); ISSN 2601 – 2332 (online); ISSN-L 1584 – 2665

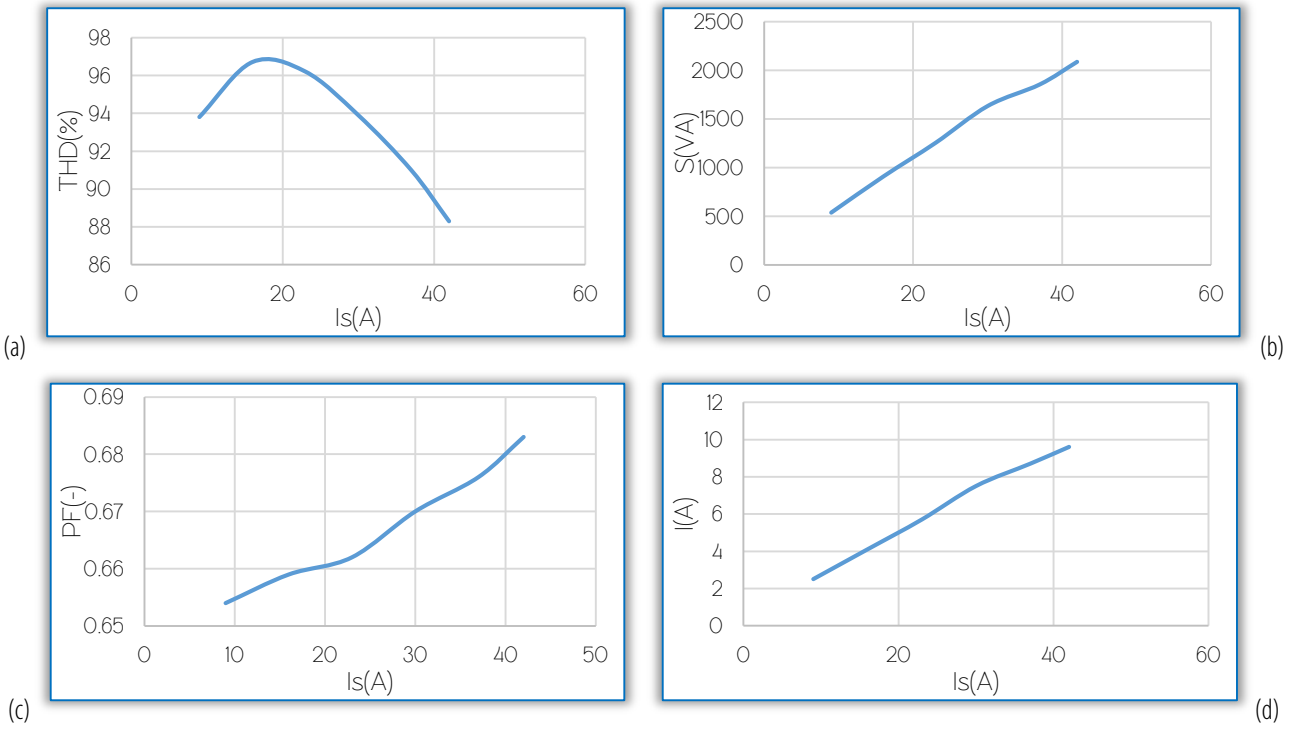

Figure 9. Graphic representations: a) THD=f(I_s); b) S=f(I_s); c) PF=f(I_s); d) I=f(I_s).

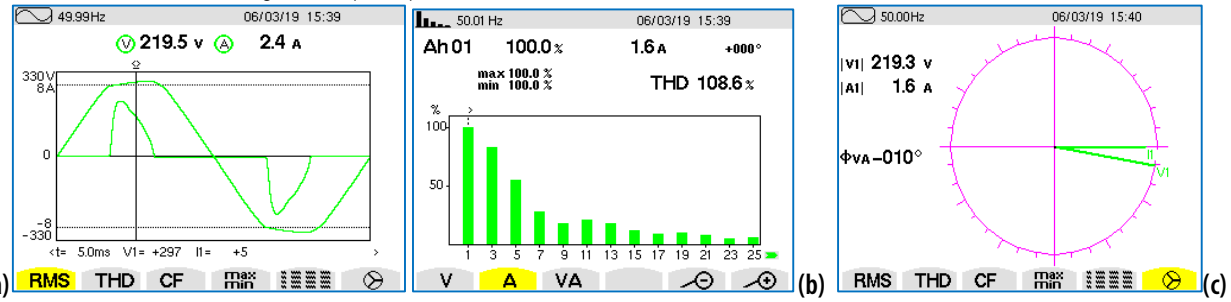

Figure 9. Measurements with CA 8334B: a) Voltage and current over a period;
b) The harmonic spectrum of the current and the total harmonic distortion factor (THD); c) Fresnel diagram for the fundamental at I_s= 9 A

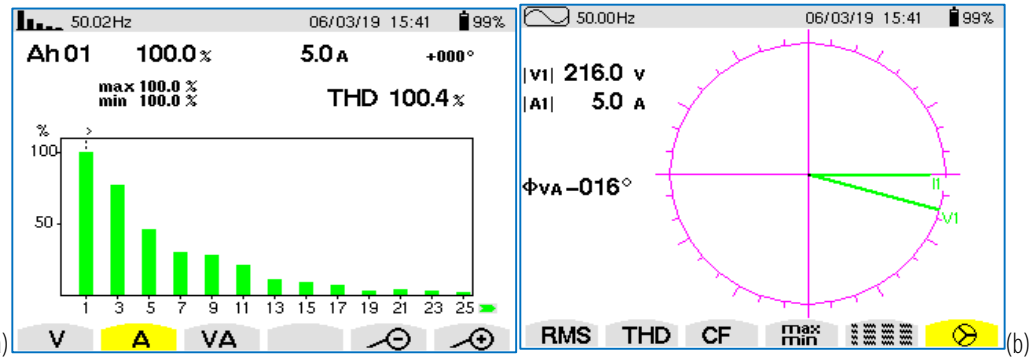

Figure 10. Measurements with CA 8334B: a) The harmonic spectrum of the current and the total harmonic distortion factor (THD);
b) Fresnel diagram for the fundamental at I_s= 30 A

— Connecting a LC shunt filter having the characteristics: RL = 1.5 Ω, L = 33.7 mH, C = 10 μF

This variant highlights the reduction of the harmonic distortion factor by approximately 10 percent compared to the situation without the connected filter, with the difference that this time it increases with the increase of the welding current (Fig.11.a). At the same time, there is a small increase in active power at the expense of reactive power, but it remains lower than the latter. The variation of the power factor PF and the displacement power factor DPF have the same direction of increase, they increase their value when the welding current increases (Table 3, Fig.11.c).

$$f = \frac{1}{2\pi\sqrt{LC}} = \frac{1}{2\pi\sqrt{33{,}7\cdot10^{-3}\cdot10\cdot10^{-6}}} = \frac{1}{2\pi\sqrt{33{,}7\cdot10\cdot10^{-9}}} = 274.24\ \text{Hz} \quad (2)$$

ISSN 1584 – 2665 (printed version); ISSN 2601 – 2332 (online); ISSN-L 1584 – 2665

Table 3–Experimental measurements made with the resistive load welding device: $R_L = 1.5\ \Omega$, with LC shunt filter, $L = 33.7$ mH, $C = 10\ \mu F$

I(A)	THD(%)	P(W)	Q(VAR)	S(VA)	PF(–)	DPF (–)	I_s(A)
2.5	87.7	348	427	550	0.632	0.859	9
4.1	95.7	577	694.5	906	0.639	0.904	16
5.8	96.9	807	968	1258	0.642	0.915	23
7.1	95.7	995	1179	1545	0.648	0.918	30
8.8	92.3	1254	1430	1912	0.662	0.922	37
8.7	91.7	1253	1420	1892	0.66	0.922	42

The reduction of the harmonic distortion factor THD can be highlighted from the representation of the current harmonic values for both the 9 A and 30 A currents (Fig.12.b and 13.b) as well as from the form of variation of voltage and current (Fig.12.a and 13.a), especially of the shape of the current. At the same time, there is a significant increase in the phase shift between voltage and current, compared to the previous situation when no filter was used.

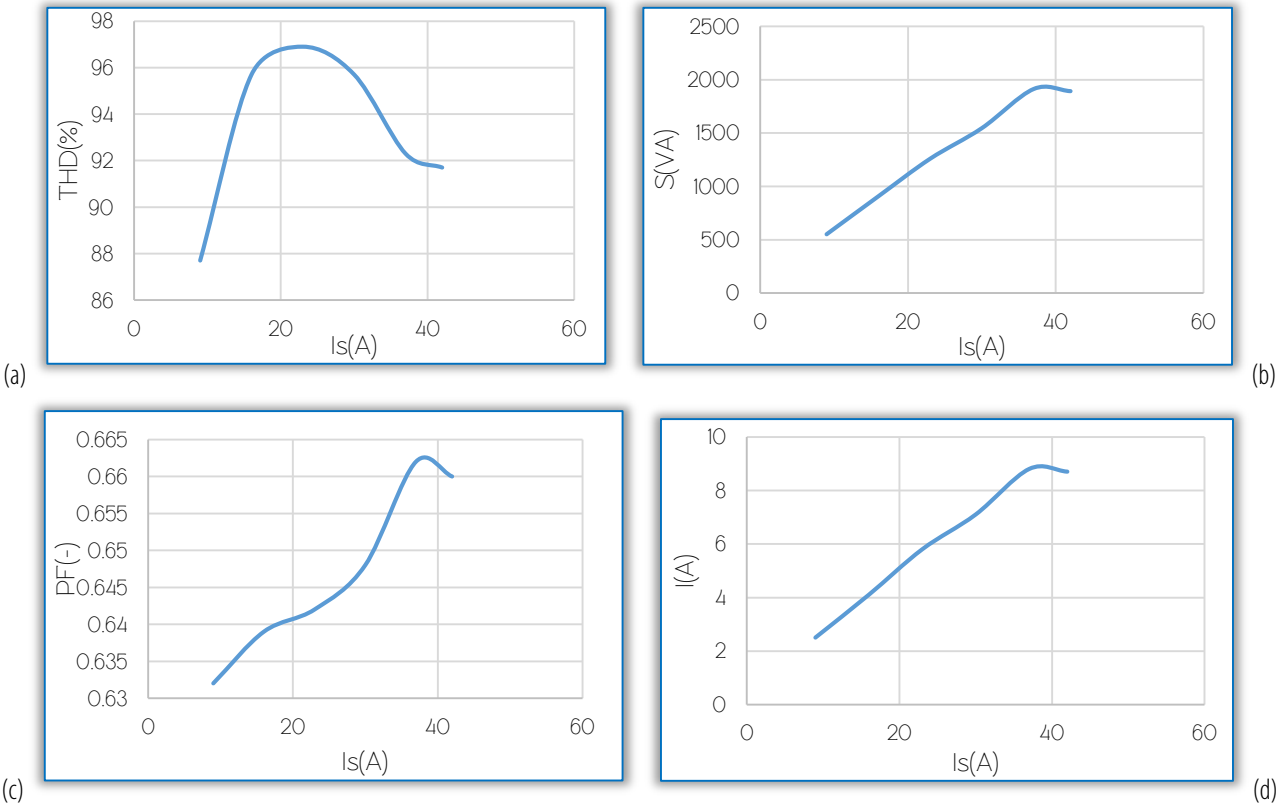

Figure 11. Graphic representations: a) THD=f(I_s); b) S=f(I_s); c) PF=f(I_s); d) I=f(I_s).

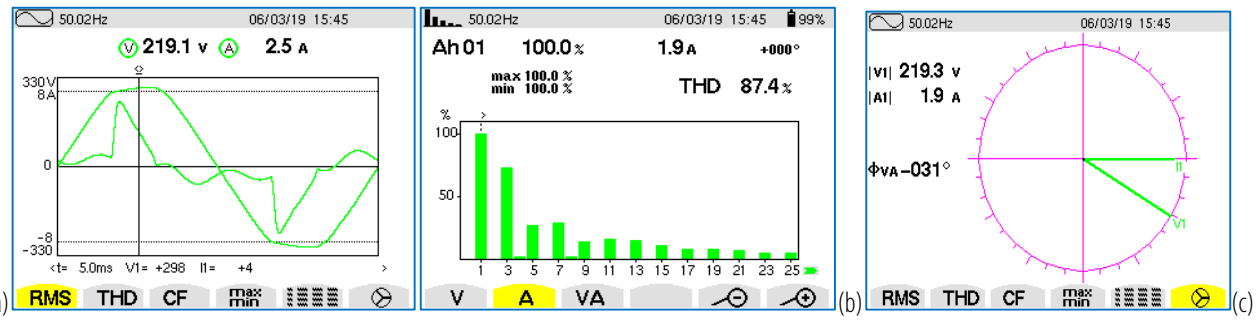

Figure 12. Measurements with CA 8334B: a) Voltage and current over a period; b) The harmonic spectrum of the current and the total harmonic distortion factor (THD); c) Fresnel diagram for the fundamental at I_s= 9 A

ISSN 1584 – 2665 (printed version); ISSN 2601 – 2332 (online); ISSN-L 1584 – 2665

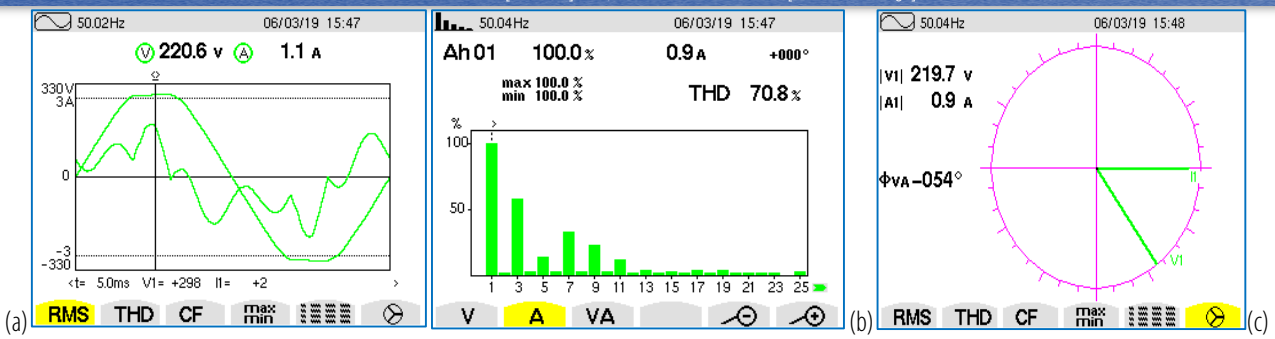

(a) (b) (c)

Figure 13. Measurements with CA 8334B: a) Voltage and current over a period; b) The harmonic spectrum of the current and the total harmonic distortion factor (THD); c) Fresnel diagram for the fundamental at I_s= 30A

— Connecting a LC shunt filter having the characteristics: R_L =1.5 Ω, L=19.9 mH, C= 15 μF

In this situation (Table 4), there is a reduction of approximately 20 percent in the THD factor and an increase in the share of active power compared to reactive power, but still lower in value than the latter. Lower values are obtained for the displacement factor DPF compared to the previously studied situations.

$$f = \frac{1}{2\pi\sqrt{LC}} = \frac{1}{2\pi\sqrt{19{,}9\cdot10^{-3}\cdot15\cdot10^{-6}}} = \frac{1}{2\pi\sqrt{19{,}9\cdot15\cdot10^{-9}}} = 291.71\text{Hz} \quad (3)$$

Table 4–Experimental measurements made with the resistive load welding device: $R_L = 1{,}5\Omega$, LC shunt filter, L=19.9 mH, C=15 μF

I(A)	THD(%)	P(W)	Q(VAR)	S(VA)	PF(–)	DPF (–)	I_s(A)
2.7	78.3	354	475	592	0.597	0.77	9
4.2	88.8	574	723	921.5	0.622	0.85	16
5.9	91.9	833	998	1300	0.636	0.883	23
7.2	90	991	1179	1542	0.647	0.893	30
8.9	88.1	1275	1444	1915	0.661	0.902	37
9.4	86.4	1358	1526	2036	0.665	0.903	42

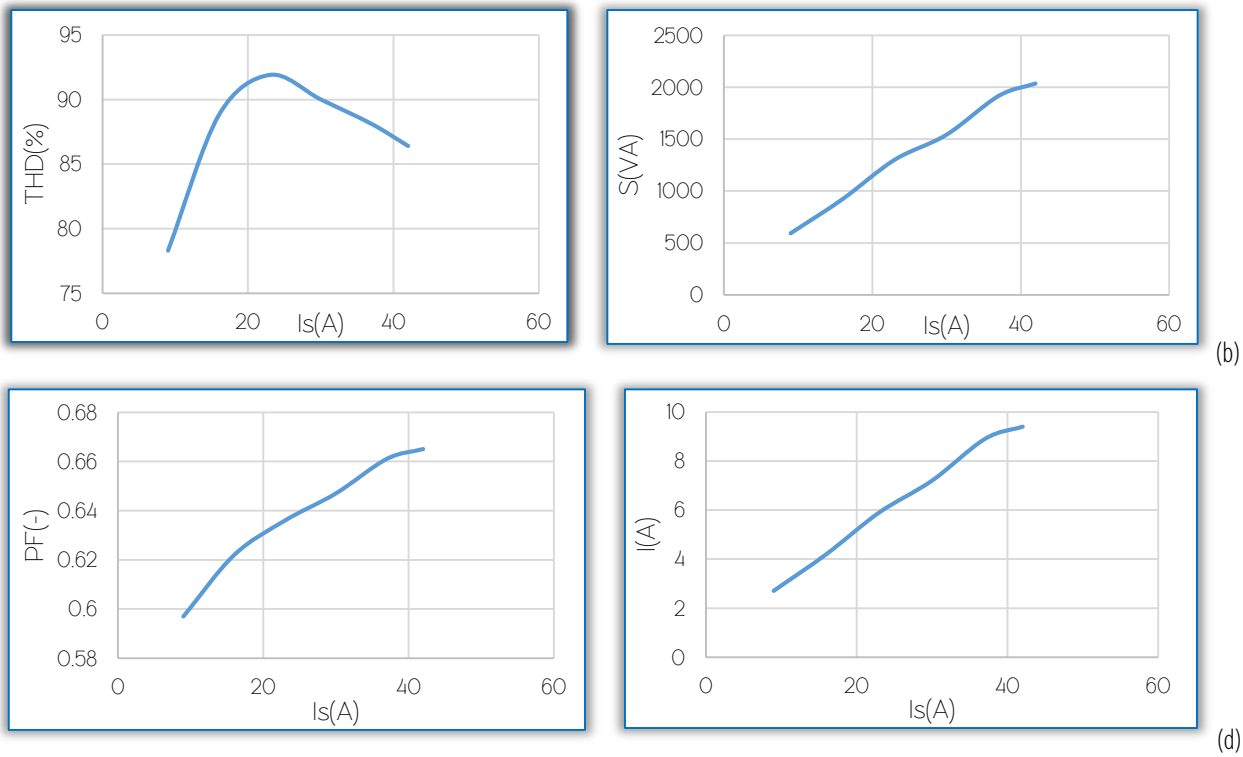

(a) (b) (c) (d)

Figure 14. Graphic representations: a) THD=f(I_s); b) S=f(I_s); c) PF=f(I_s); d) I=f(I_s).

The reduction of the total harmonic distortion factor THD can also be observed in Figs. 15 and 16, where the current waveform begins to approach a sinusoidal shape, the harmonics are reduced, especially the 5th order one, and the phase shift continues to increase by almost the same percentage as in previous cases.

ISSN 1584 – 2665 (printed version); ISSN 2601 – 2332 (online); ISSN-L 1584 – 2665

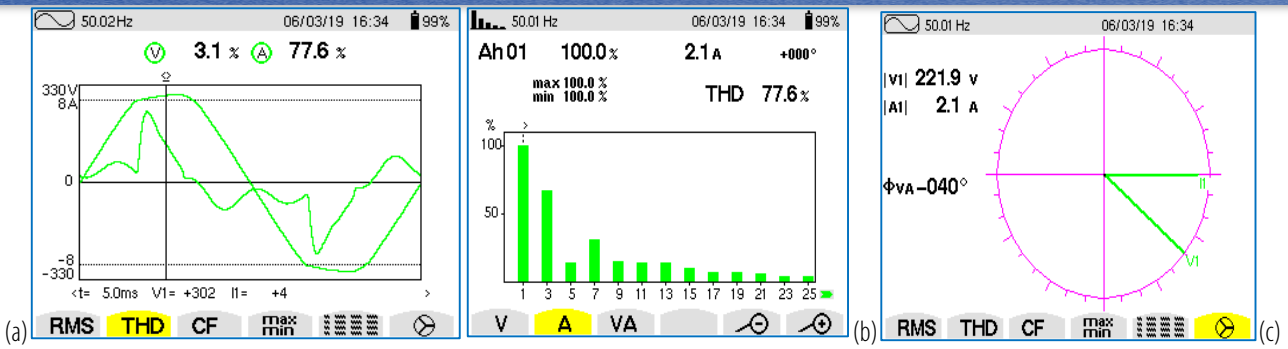

Figure 15. Measurements with CA 8334B: a) Voltage and current over a period;
b) The harmonic spectrum of the current and the total harmonic distortion factor (THD); c) Fresnel diagram for the fundamental at I_s= 9A

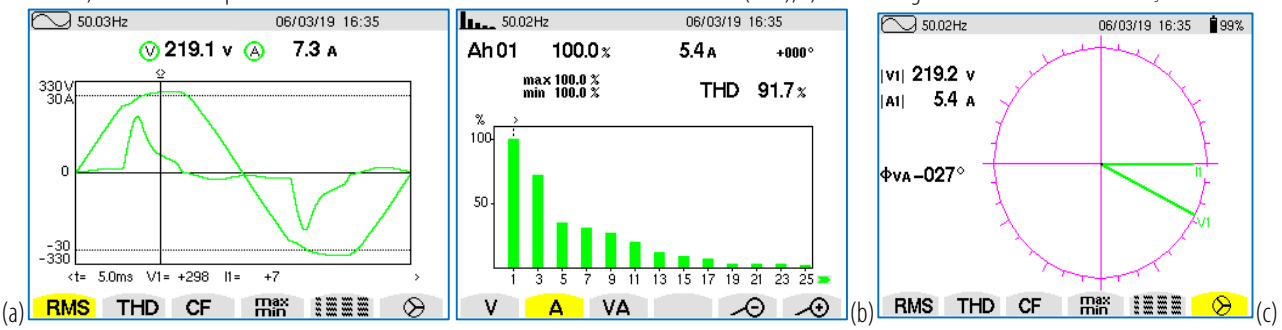

Figure 16. Measurements with CA 8334B: a) Voltage and current over a period;
b) The harmonic spectrum of the current and the total harmonic distortion factor (THD); c) Fresnel diagram for the fundamental at I_s= 30A

— Connecting an LC shunt filter having the characteristics: R_L = 1.5 Ω, L = 13.4 mH, C = 20 μF

In this case, values lower by approximately 20% compared to the initial situation of the total harmonic distortion factor (THD) are obtained, the reactive power remains higher than the active one which kept the increasing trend, but with little important values compared to the reactive power. PF and DPF have the same tendency to increase with the increase of the welding current and with significantly lower values than the previous case (Fig.17.c).

$$f = \frac{1}{2\pi\sqrt{LC}} = \frac{1}{2\pi\sqrt{13{,}4\cdot10^{-3}\cdot20\cdot10^{-6}}} = \frac{1}{2\pi\sqrt{13{,}4\cdot20\cdot10^{-9}}} = 307.69\ \text{Hz} \quad (4)$$

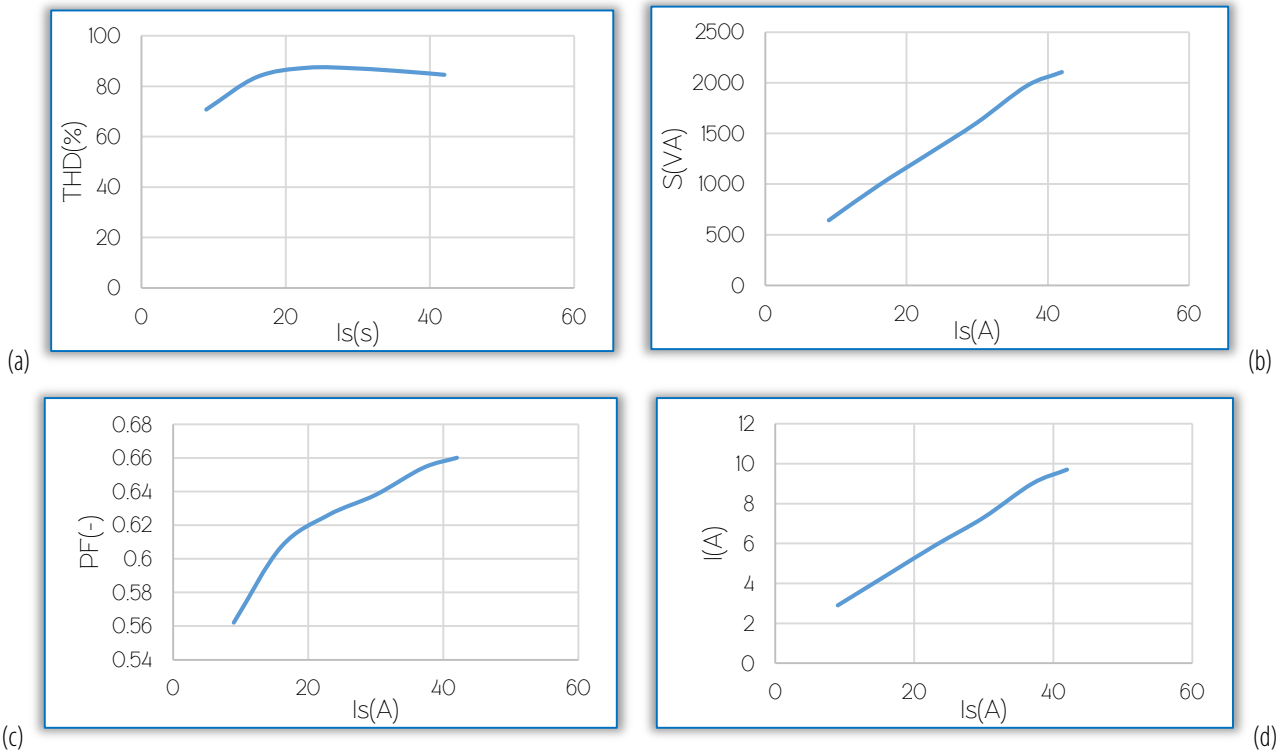

Figure 17. Graphic representations: a) THD=f(I_s); b) S=f(I_s); c) PF=f(I_s); d) I=f(I_s).

ISSN 1584 – 2665 (printed version); ISSN 2601 – 2332 (online); ISSN-L 1584 – 2665

Table 5–Experimental measurements made with the resistive load welding device: $R_L = 1.5\ \Omega$, with LC shunt filter, $L = 13.4$ mH, $C = 20\ \mu F$

I(A)	THD(%)	P(W)	Q(VAR)	S(VA)	PF(–)	DPF(–)	I_s(A)
2.9	70.7	361	532	643	0.562	0.7	9
4.4	83.6	597.6	784	985.1	0.607	0.807	16
5.9	87.3	810	1010	1294	0.626	0.847	23
7.3	87	1025	1236	1607	0.638	0.867	30
9	85.7	1285	1486	1968	0.654	0.882	37
9.7	84.5	1388	1582	2105	0.66	0.886	42

These effects can, also, be seen from Figs.18.a and 19.a, where the shape of the current variation starts to be closer to the sinusoidal one, and the values of the harmonics are significantly reduced. The phase shift changes the direction of variation, it has a smaller value at a higher current (30 degrees at a current of 30 A, compared to 45 degrees at 9 A, Figs.18.c and 19.c).

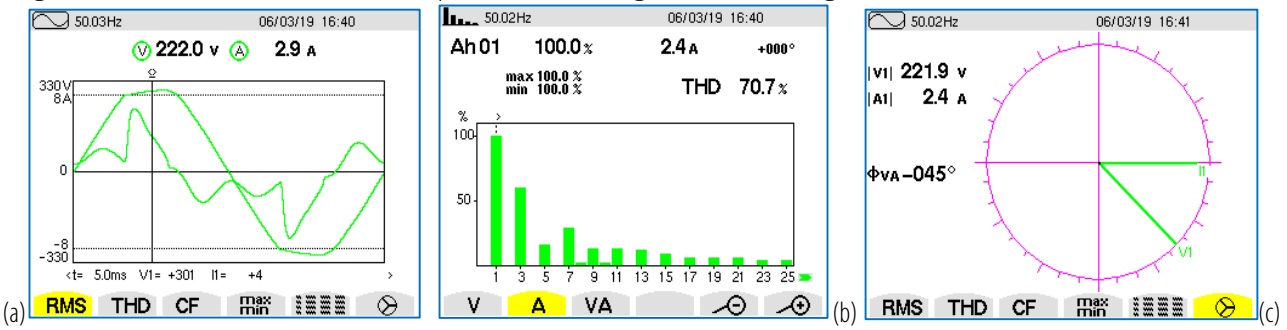

Figure 18. Measurements with CA 8334B: a) Voltage and current over a period;
b) The harmonic spectrum of the current and the total harmonic distortion factor (THD); c) Fresnel diagram for the fundamental at I_s= 9A

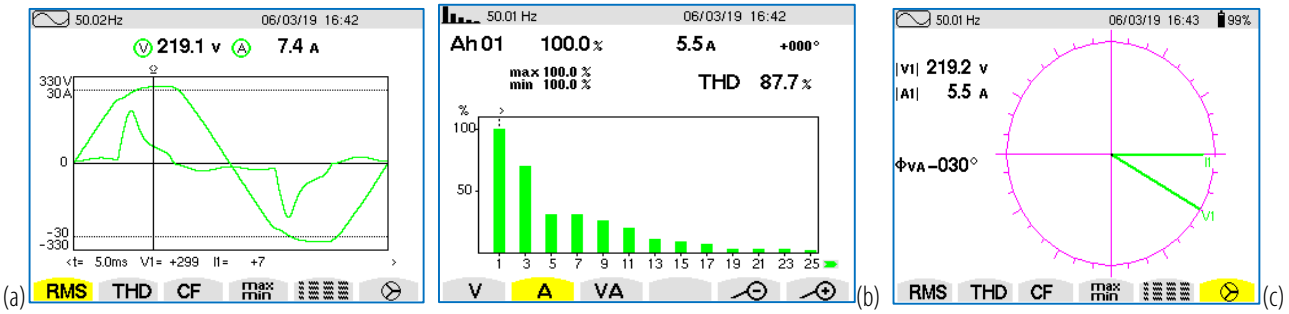

Figure 19. Measurements with CA 8334B: a) Voltage and current over a period;
b) The harmonic spectrum of the current and the total harmonic distortion factor (THD); c) Fresnel diagram for the fundamental at I_s= 30A

The welding machine was connected with a capacitive filter connected in parallel (Fig. 20).

The use of a capacitive filter brings us back close to the situation with the LC filter tuned to 136 Hz [13]. The values are close, as can be seen both from the value tables and from the variations in the waveforms for voltage and current, as well as from the current harmonic values. For phase shift, an inversion of values is observed, meaning that at a higher current, a lower phase shift is obtained compared to a lower output current.

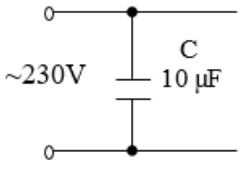

Figure 20. Capacitive filter

Table 6–Experimental measurements made with the resistive load welding machine: $R_L = 1.5\ \Omega$, with a capacitive filter, $C = 10\ \mu F$

I(A)	THD (%)	P (W)	Q (VAR)	S (VA)	PF (–)	DPF (–)	Is (A)
2.5	89.7	361.6	443.5	574	0.629	0.87	9
4.2	96	600.3	720	939.1	0.643	0.911	16
5.8	96.1	839	989	1296	0.646	0.922	23
7.1	94	1042	1196	1588	0.657	0.926	30
8.8	90.6	1301	1452	1945	0.669	0.927	37
9.3	89	1394	1524	2064	0.675	0.928	42

ISSN 1584 – 2665 (printed version); ISSN 2601 – 2332 (online); ISSN-L 1584 – 2665

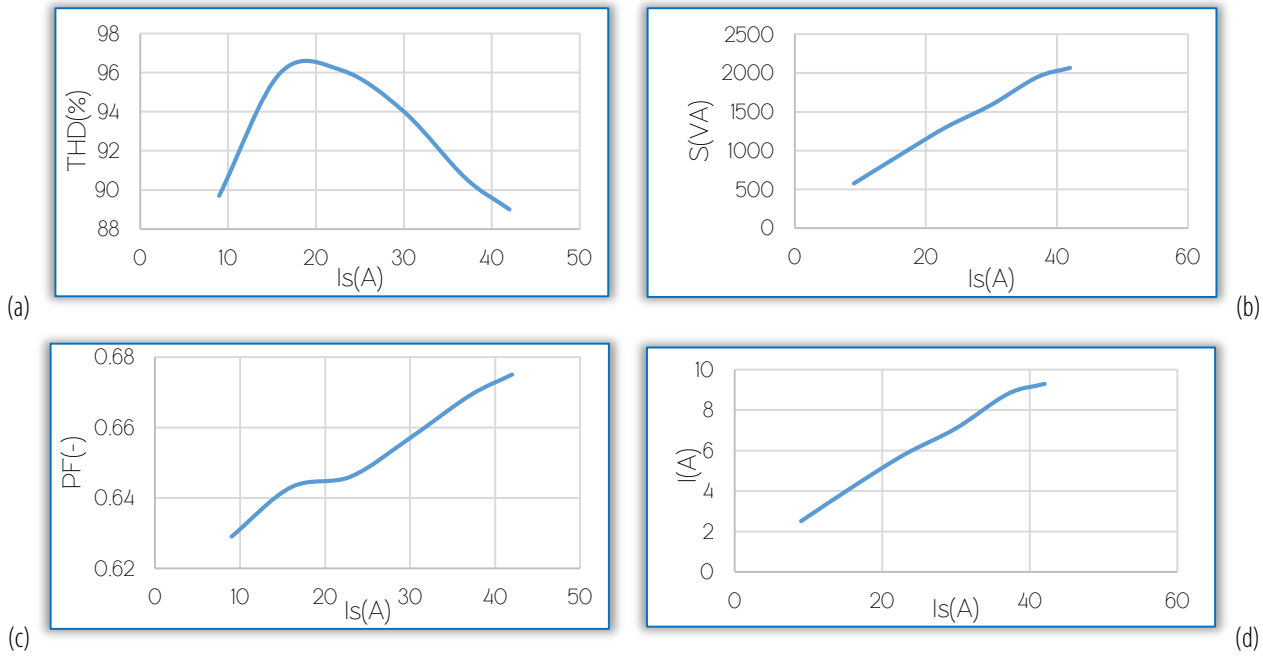

(a) (b) (c) (d)

Figure 21. Graphic representations: a) THD=f(I_s); b) S=f(I_s); c) PF=f(I_s); d) I=f(I_s).

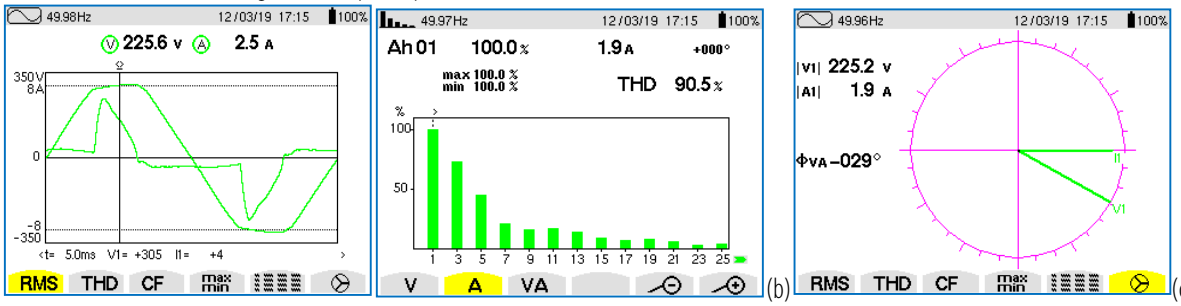

(a) (b) (c)

Figure 22. Measurements with CA 8334B: a) Voltage and current over a period; b) The harmonic spectrum of the current and the total harmonic distortion factor (THD); c) Fresnel diagram for the fundamental at I_s= 9A

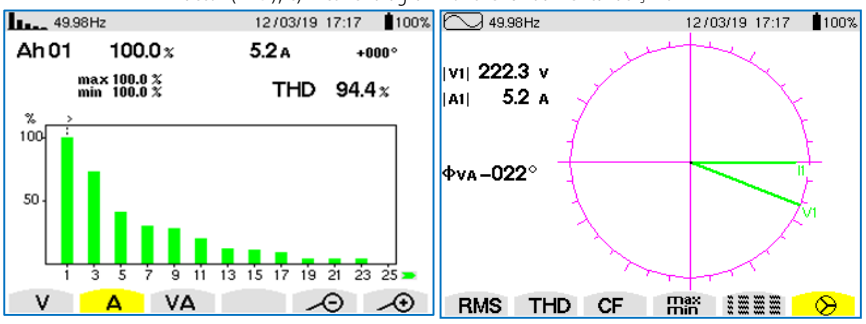

(a) (b)

Figure 22. Measurements with CA 8334B: a) The harmonic spectrum of the current and the total harmonic distortion factor (THD); b) Fresnel diagram for the fundamental at I_s= 30A

4. CONCLUSIONS

In the experimental analysis of LC shunt filters, a non–linear consumer that is often found in practice was used, a single–phase manual welding machine type XENTA 90.

Tuning the LC shunt filters to a certain harmonic is nearly impossible, being difficult to calibrate L. At the same time, the impedance of the source influences the performance of the filter. When LC shunt filters are used, the AC current from the network can increase by 5%, compared to the situation without passive filters.

For this type of consumer, there are decreasing harmonics along with the rank of the harmonics, the best filtering is performed with tuned filters close to the harmonic of order 3 to 5; filters above this value are no longer as effective. Compared to the situation in which no filters are used, by using LC shunt filters, THD for current decreases, P increases slightly, PF decreases slightly, and DPF decreases considerably (especially when using large filtering capacities).

ISSN 1584 – 2665 (printed version); ISSN 2601 – 2332 (online); ISSN-L 1584 – 2665

References

[1] Power Quality Application Guide. Available online: https://www.sier.ro/ghid_aplicare.html
[2] A.A. El–Ela, S.M. Allam, A.A. Mubarak, R.A. El–Sehiemy, "Harmonic Mitigation by Optimal Allocation of Tuned Passive Filter in Distribution System," Energy Power Eng. 2022, 14, 291–312.
[3] R.S. Widagdo, A.H. Andriawan, R. Hartayu, "Harmonic Mitigation in Microgrids to Improve Power Quality" J. Teknol. Elektro 2024, 15, 11–19.
[4] A.A. Abou El–Ela , S. Allam , H. El–Arwash "An Optimal Design Of Single Tuned Filter In Distribution Systems I" Electric Power Systems Research 78 (2008) 967–974.
[5] T.M.T. Thentral, S. Usha, R. Palanisamy, A. Geetha, A.M. Alkhudaydi, N.K. Sharma, M. Bajaj, S.S.M. Ghoneim, M. Shouran, S. Kamel, "An energy efficient modified passive power filter for power quality enhancement in electric drives" Front. Energy Res. 2022, 10, 1–20.
[6] R. Sirjani, B. Hassanpou" A New Ant Colony–Based Method for Optimal Capacitor Placement and Sizing in Distribution Systems" Research Journal of Applied Sciences, Engineering and Technology 4(8): 888–891, 2012.
[7] S.A. Sahidaini, "Electrical Power Quality Improvement through Modeling and Optimization of Passive Harmonic Filter" International Journal of Engineering Research & Technology (IJERT) ISSN: 2278–0181, Vol. 7 Issue 10, October–2018.
[8] O. A. Monem "Harmonic mitigation for power rectifier using passive filter combination" IOP Conf. Series: Materials Science and Engineering 610 (2019) 012013, IOP Publishing.
[9] Z. A. Memon, M. A. Uquaili, A.M. A. Unar, "Harmonics Mitigation of Industrial Power System Using Passive Filters", Mehran University Research Journal of Engineering & Technology, Volume 31, No. 2, April, 2012 [ISSN 0254–7821].
[10] S.Rüstemli, E.Okuducu, M.N.Almali, S. B. Efe, "Reducing the effects of harmonics on the electrical power systems with passive filters" Bitlis Eren Univ J Sci & Technol 5 (1), 1 – 10, 2015.
[11] M. A. Soomro, A. A. Sahito, I. A. Halepoto, K. Kazi, "Single Tuned Harmonic Shunt Passive Filter Design for Suppressing Dominant Odd Order Harmonics in order to Improve Energy Efficiency" Indian Journal of Science and Technology, Vol 9(47), December 2016.
[12] M.M. Ishaya, O.R. Adegboye, E.B. Agyekum, M.F. Elnaggar, M.M. Alrashed, S. Kamel, "Single–tuned passive filter (STPF) for mitigating harmonics in a 3–phase power system" Sci. Rep. 2023, 13, 20754.
[13] C.S. Azebaze Mboving, "Investigation on the Work Efficiency of the LC Passive Harmonic Filter Chosen Topologies" Electronics, 2021, 10, 896.
[14] G.N. Popa, A. Iagăr, C.M. Diniș, "Considerations on Current and Voltage Unbalance of Nonlinear Loads in Residential and Educational Sectors," Energies 2021, 14, 102.
[15] B. Park, J. Lee, H. Yoo, G. Jang, "Harmonic Mitigation Using Passive Harmonic Filters: Case Study in a Steel Mill Power System," Energies 2021, 14, 2278.
[16] T.Meng, H. Ben, Y. Song, C. Li,"Analysis and Design of an Input–Series Two–Transistor Forward Converter For High–Input Voltage Multiple–Output Applications" IEEE Transactions On Industrial Electronics, Vol. 65, No. 1, January 2018.

ISSN 1584 – 2665 (printed version); ISSN 2601 – 2332 (online); ISSN-L 1584 – 2665